MOLECULAR AND CELLULAR BIOLOGY, Feb. 1996, p. 634–647 Vol. 16, No. 2
0270-7306/96/$04.00+0

Protein-DNA Interactions at the Major and Minor Promoters of the Divergently Transcribed *dhfr* and *rep3* Genes during the Chinese Hamster Ovary Cell Cycle

JULIE WELLS,[1,2] PAUL HELD,[2]† SHARON ILLENYE,[2] AND NICHOLAS H. HEINTZ[1,2]*

Program in Cell and Molecular Biology[1] and Department of Pathology,[2] University of Vermont College of Medicine, Burlington, Vermont 05405

Received 19 September 1995/Accepted 15 November 1995

In mammals, two TATA-less bidirectional promoters regulate expression of the divergently transcribed dihydrofolate reductase (*dhfr*) and *rep3* genes. In CHOC 400 cells, *dhfr* mRNA levels increase about fourfold during the G_1-to-S phase transition of the cell cycle, whereas the levels of *rep3* transcripts vary less than twofold during this time. To assess the role of DNA-binding proteins in transcriptional regulation of the *dhfr* and *rep3* genes, the major and minor *dhfr-rep3* promoter regions were analyzed by high-resolution genomic footprinting during the cell cycle. At the major *dhfr* promoter, prominent DNase I footprints over four upstream Sp1 binding sites did not vary throughout G_1 and entry into the S phase. Genomic footprinting revealed that a protein is constitutively bound to the overlapping E2F sites throughout the G_1-to-S phase transition, an interaction that is most evident on the transcribed template strand. On the nontranscribed strand, multiple changes in the DNase I cleavage pattern are observed during transit through G_1 and entry into the S phase. By using gel mobility shift assays and a series of sequence-specific probes, two different species of E2F were shown to interact with the *dhfr* promoter during the cell cycle. The DNA binding activity of one E2F species, which preferentially recognizes the sequence TTTGGCGC, did not vary significantly during the cell cycle. The DNA binding activity of the second E2F species, which preferentially recognizes the sequence TTTCGCGC, increased during the G_1-to-S phase transition. Together, these results indicate that Sp1 and the species of E2F that binds TTTGGCGC participate in the formation of a basal transcription complex, while the species of E2F that binds TTTCGCGC regulates *dhfr* gene expression during the G_1-to-S phase transition. At the minor promoter, DNase I footprints at a consensus c-Myc binding site and three Sp1 binding sites showed little variation during the G_1-to-S phase transition. In addition to protein binding at sequences known to be involved in the regulation of transcription, genomic footprinting of the entire promoter region also showed that a protein factor is constitutively bound to the first intron of the *rep3* gene.

Transition through the eucaryotic cell cycle is accompanied by the periodic expression of gene products that participate in cell cycle-dependent processes such as DNA replication and mitosis. The transcription of several genes involved in entry into the S phase and DNA replication, including the dihydrofolate reductase (*dhfr*), DNA polymerase α, thymidine kinase, and *cdc2* genes, increases as cells transit through G_1 and enter the S phase (reviewed in references 26, 42, and 59). Of these genes, the control of transcription during the cell cycle has been examined most thoroughly for the *dhfr* gene (reviewed in references 2, 26, and 59). The transcription of *dhfr* is low in serum-deprived or quiescent cells, increases as cells transit through the G_1 phase, and reaches maximal levels late in G_1 or early in the S phase (22–24, 29, 30, 37, 57, 58, 61). Sequence comparisons show that the *dhfr* promoter regions of hamsters, mice, and humans share a number of conserved features. The promoters are GC rich and devoid of obvious TATA boxes and contain consensus sequences for several *trans*-acting transcription factors (2, 49, 59).

Promoter dissection studies have shown that a 70-bp region encompassing the major transcription start site from either the mouse or the Chinese hamster *dhfr* gene confers growth-dependent transcription on heterologous reporter genes (47, 65). The minimal promoter region includes at least three elements important for regulating transcription, binding sites for the transcription factor Sp1 (7, 12, 25, 47, 64, 66), structural control elements (SCEs) that may reduce the frequency of transcription initiation (54), and two overlapping binding sites for the heterodimeric transcription factor E2F (6, 47, 63). Promoter reconstruction studies indicate that overlapping binding sites for E2F are critical for growth-dependent increases in *dhfr* transcription (63), as well as the periodic expression of at least one member of the E2F gene family, E2F-1 (34, 37, 51). Thus, at the major *dhfr* promoter, Sp1 may be involved in promoter recognition and the establishment of a basal transcription complex, while E2F may regulate induction of transcription during the transition of G_1 and entry into the S phase.

Transcript mapping has revealed the presence of a second, divergent transcription unit upstream of the *dhfr* gene (here referred to as *rep3*) that encodes a homolog of the bacterial mismatch repair protein MutS (14, 45, 49, 55). *rep3* and *dhfr* transcripts arise from multiple start sites within a 500- to 800-bp region that includes two clusters of Sp1 sites oriented in opposite directions (14, 45, 49, 60). Ninety percent of the *dhfr* transcripts and a majority of *rep3* transcripts arise from the cluster of Sp1 sites associated with the major *dhfr* promoter (7, 14, 45, 46, 49, 65). The remainder of transcripts for both genes begin at a minor TATA-less promoter associated with the distal cluster of Sp1 sites (14, 45, 49, 60). The minor promoter

* Corresponding author. Mailing address: Department of Pathology, Soule Medical Alumni Building, University of Vermont College of Medicine, Burlington, VT 05405. Phone: (802) 656-2210. Fax: (802) 656-8892. Electronic mail address: nheintz@moose.uvm.edu.

† Present address: Bio-Tek Instruments Inc., Winooski, VT 05404-0998.

lies within the first intron of a primary *rep3* mRNA that is transcribed from the major promoter in the opposite direction from *dhfr* (45, 60; also see Fig. 2). Thus, the *dhfr-rep3* promoter region contains two overlapping bidirectional promoters, each of which contributes to the expression of both genes. Although the role of *rep3* in DNA metabolism is not known, the unusual organization of the *dhfr-rep3* promoter region is very highly conserved in mammals (reviewed in references 2 and 59), indicating that coordinate regulation of these two genes may be physiologically important.

To address the role of DNA-binding proteins in the regulation of *dhfr* gene expression, particularly in regard to the G_1-to-S phase transition of the cell cycle, a high-resolution genomic footprinting technique was used to examine protein-DNA interactions throughout the bidirectional promoter region during the cell cycle. To facilitate these footprinting studies, we used a methotrexate-resistant cell line, CHOC 400, that contains approximately 1,000 copies of the *dhfr* and *rep3* genes (48). The amplified *dhfr* genes of CHOC 400 cells are active; these cells produce approximately 1,000 times the levels of *dhfr* mRNA and protein that methotrexate-sensitive CHO cells do (48). Our results indicate that Sp1 and the species of E2F which binds at the primary transcription initiation site of the *dhfr* gene establish a basal transcription complex at the major promoter in early G_1 and that the species of E2F that preferentially recognizes the sequence TTTCGCGC at the overlapping E2F sites regulates growth-dependent increases in the transcription of *dhfr* during the G_1-to-S phase transition. At the minor promoter, Sp1 and c-Myc appear to form a transcription complex that persists throughout the early cell cycle. In addition, we find that all major DNase I sites mapped in this region by others coincide with sequences occupied by *trans*-acting DNA-binding proteins.

MATERIALS AND METHODS

Cell culture and synchrony. CHOC 400 cells were grown in 5% CO_2 at 37°C in Dulbecco modified Eagle medium (Mediatech) supplemented with 5% fetal bovine serum (Gibco BRL). For synchronization, cells were plated at 50 to 60% confluence and then collected in G_0/G_1 by incubation in isoleucine-free modified Eagle medium (Select-Amine; Gibco BRL) for 45 h (18). For mid-G_1 cells, G_0/G_1 cultures were washed twice with phosphate-buffered saline (PBS) and then incubated in complete medium with 5% serum for 2 h. For G_1/S cells, cultures arrested in G_0 by isoleucine deprivation were incubated in complete medium plus serum containing 400 μM mimosine (Sigma) for 14 h (18). Early-S-phase cells were obtained by washing cells arrested at the G_1/S boundary with serum-free medium three times, with subsequent incubation in Dulbecco modified Eagle medium with serum for 2 h. Cell fractions enriched for cells in mitosis were obtained with Colcemid by the method of Stubblefield and Klevecz (65). Flow cytometry shows that under these synchrony conditions, about 82% of the cells in G_0 culture, 81% of the cells in G_1 culture, and 84% of the cells in G_1/S cultures have a 2 N DNA content (data not shown). By 2 h after release from the G_1/S mimosine block, at least 65% of the cells detected are in the S phase. About 40 to 45% of the mitotic cell fractions displayed a 4 N DNA content; the remainder of cells after Colcemid block were distributed throughout the cell cycle.

Northern (RNA) blot analysis. Total cellular RNA was isolated, resolved by electrophoresis, and transferred to nitrocellulose membranes as previously described (62). Northern blots were probed with murine *dhfr* cDNA sequences from plasmid ΔVa-pMT2 and murine *rep3* cDNA sequences from plasmid pGC1587 that had been radiolabeled with ^{32}P-deoxynucleoside triphosphates (dNTPs), as previously described (62). After being washed, hybridization signals were visualized by autoradiography and quantified with a Bio-Rad GS-250 Molecular Imager.

Genomic footprinting. Templates for genomic footprinting were prepared from synchronized cells by a procedure modified from that of Pfeifer and Riggs (53). Briefly, cells were washed with solution 2 (150 mM sucrose, 80 mM KCl, 35 mM HEPES [*N*-2-hydroxyethylpiperazine-*N*′-2-ethanesulfonic acid] [pH 7.4], 5 mM K_2HPO_4, 5 mM $MgCl_2$, 2 mM $CaCl_2$) and then treated with solution 2 containing 0.05% lysophosphatidylcholine (Sigma) and 2.5 to 20 μg of DNase I (Gibco BRL) per ml for 6 min. The reaction was stopped by the addition of 5× stop buffer (50 mM Tris-HCl [pH 8.0], 425 mM NaCl, 62.5 mM EDTA, 2.5% sodium dodecyl sulfate, 1.5 mg of proteinase K per ml). Cell lysates were incubated at 50°C for at least 3 h and then extracted repeatedly with phenol-chloroform-isoamyl alcohol and chloroform-isoamyl alcohol. Nucleic acids were precipitated with NaCl and ethanol, treated with 100 μg of RNase A per ml, and digested with *Eco*RI. Samples were then extracted with phenol-chloroform-isoamyl alcohol and chloroform-isoamyl alcohol, and the aqueous phase was precipitated with NaCl and ethanol. Control samples cleaved with DNase I in vitro were prepared in an identical fashion, except that DNase I was added at 1.67 to 13 ng/ml in solution 2 for 6 min after the second organic extraction and ethanol precipitation. In vitro DNase I digests were stopped by the addition of phenol-chloroform-isoamyl alcohol. Genomic DNA digested with *Eco*RI but not treated with DNase I was prepared as described above, except that DNase I was omitted from the purification procedure. The extent of nuclease cleavage was determined by electrophoresis on 1% agarose gels containing ethidium bromide, and samples displaying average lengths of 1 to 5 kb were used for primer extension. Samples cleaved with DNase I to similar extents in vitro and in permeabilized cells were compared directly.

Genomic footprinting was performed by a modified primer extension assay (10). Nuclease cleavage sites were detected by reiterative primer extension with *Taq* DNA polymerase (BRL) and oligonucleotide primers end labeled with [γ-^{32}P]ATP (6,000 Ci/mmol; Dupont NEN) and polynucleotide kinase (New England Biolabs). Primer extension reaction mixtures (50 μl) contained 10 μg of DNA template, 1 pmol of labeled primer, 2.5 U of *Taq* polymerase, 1× *Taq* buffer from the supplier, 1.5 mM $MgCl_2$, and 300 μM each dNTP (Pharmacia). Primer extensions were performed in a Perkin-Elmer 9600 thermocycler for 30 cycles. The first cycle consisted of 94°C for 5 min, the melting temperature of the primer for 5 min, and 76°C for 3 min. For the next 29 cycles, the 94°C incubation was shortened to 1 min. The final cycle was followed by incubation at 76°C for 7 min. The reaction products were precipitated with ethanol, dissolved in loading buffer, and resolved on denaturing urea–10% polyacrylamide gels. Primer extension products were visualized by exposing dried gels to X-Omat film (Kodak) for 1 to 3 days without intensifying screens. The sequences of the individual oligonucleotide primers are as follows: 477, 5′-CATCGCAGGATGCAGAAG AGCAAGCCCGCCGGGA-3′; 492, 5′-CCGATGCCCATATTCTGGGACAC GGCGACGATGCA-3′; 557, 5′-CTCTGATGTTCAAATAGGATGCTAGGC TTG-3′; 561, 5′-GGCTCGTTACTCTACTCCACTTCCGGGCGC-3′; 717, 5′-CACGGACCCACGGATGTCACCCACT-3′; 718, 5′-CCGGCGGGCTTGCTC TTCTGCATCC-3′.

Gel mobility shift assays. Gel mobility shift assays were performed with whole-cell extracts and end-labeled double-stranded oligonucleotide probes (33). For whole-cell extracts, cells were washed twice with PBS and scraped into a microcentrifuge tube. For each 50 μl of cells, 200 μl of 5× 500 buffer (100 mM HEPES [pH 7.4], 500 mM KCl, 5 mM $MgCl_2$, 0.5 mM EDTA, 35% glycerol, 5 mM NaF, 2 μg of phenylmethylsulfonyl fluoride per ml, 0.1 μg of aprotinin per ml, 0.1 μg of leupetin per ml, 1 mM dithiothreitol) was added. Samples were freeze-thawed in liquid nitrogen three times, cooled at 4°C for 30 min, and spun at 300,000 × *g* for 15 min at 4°C. For standard binding reaction mixtures, an equal amount of extract from each supernatant was incubated with 1 μg of herring sperm DNA for 10 min at room temperature, 1 ng of labeled probe and 50 ng of specific competitor DNA (if used) were added, and reaction mixtures were incubated at room temperature for an additional 20 min. Protein-DNA complexes were resolved on 4% nondenaturing polyacrylamide gels in 0.25× Tris-borate-EDTA at 4°C. After the gel was dried, protein-DNA complexes were visualized by autoradiography.

RESULTS

Expression of *dhfr* during the G_1-to-S phase transition. CHOC 400 cells are resistant to methotrexate because of the expression of high levels of *dhfr* mRNA and protein from amplified copies of the *dhfr* gene (48). To determine if *dhfr* and *rep3* mRNA levels fluctuate during the CHOC 400 cell cycle, CHOC 400 cells were first collected in G_0/G_1 by isoleucine deprivation (reference 18 and references therein) and then induced to reenter the cell cycle by the addition of complete medium. Cells were also collected at the G_1/S boundary or in S phase with a mimosine block (18). Total RNA was collected from synchronized cells and analyzed for *dhfr* and *rep3* mRNAs by Northern blotting. As shown in Fig. 1A and C, the abundance of the major *dhfr* mRNA of approximately 2,300 bases increased about three- to fourfold as cells exited G_0/G_1, traversed G_1, and entered the S phase. The levels of minor mRNA species of 1,850 and 1,100 bases that hybridized to the *dhfr* cDNA probe also increased during the G_1-to-S phase transition (Fig. 1A). The levels of all three *dhfr* transcripts decreased during the S phase (Fig. 1A and C). Thus, as observed in methotrexate-sensitive hamster, human, and murine

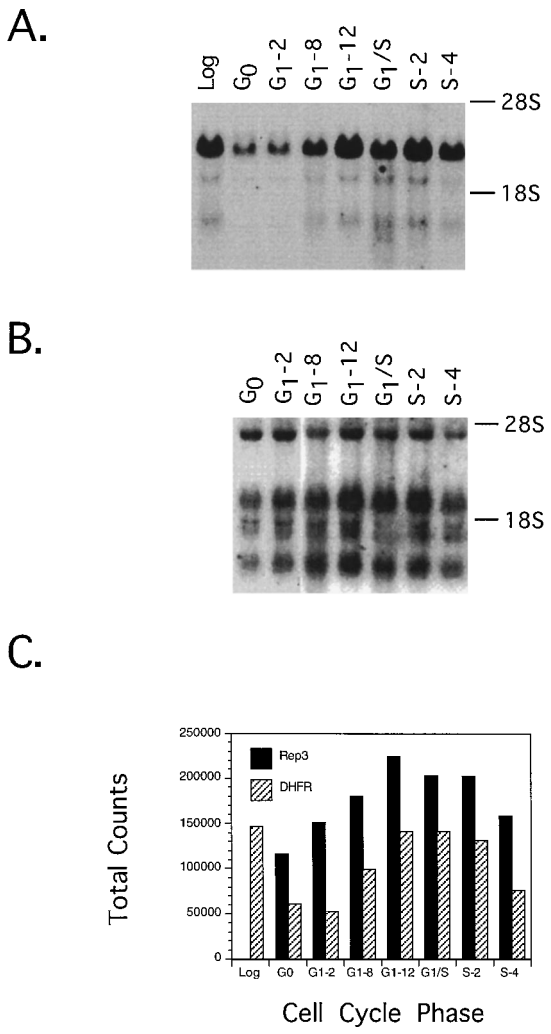

FIG. 1. Levels of *dhfr* and *rep3* mRNAs during the CHOC 400 cell cycle. Northern blots of total RNA isolated from CHOC 400 cells in log-phase growth (Log) or synchronized at various stages of the cell cycle were probed for *dhfr* (A) and *rep3* (B) mRNAs. (C) Total counts (in counts per minute per lane) in the specific hybridization signals for both groups of mRNAs. G_0, cells arrested in early G_1 by isoleucine deprivation; G_1-2, -8, and -12, cells released from the isoleucine block by the addition of complete medium for 2, 8, and 12 h, respectively; G_1/S, cells arrested at the G_1/S boundary with mimosine; S-2 and -4, cells released from the G_1/S mimosine block into S phase for 2 and 4 h, respectively.

cell lines (reviewed in reference 59), *dhfr* mRNA accumulates in CHOC 400 cells during the G_1-to-S phase transition.

Northern blot analysis also shows that CHOC 400 cells express five RNA species ranging in size from about 800 to 4,000 bases that hybridize to a murine *rep3* cDNA probe (Fig. 1B). In contrast to *dhfr* mRNA, these transcripts showed less than a twofold fluctuation in abundance during the G_1-to-S phase transition in synchronized cells (Fig. 1B and C). The relative amount of each *rep3* transcript also appears to be relatively stable under these synchrony conditions (Fig. 1B). While little is known about the regulation of *rep3* transcription (45, 49, 59, 60), present models for the regulation of *dhfr* expression during the cell cycle predict that the interaction of E2F with *dhfr* promoter sequences may change during traversal of G_1 and entry into the S phase, while Sp1 would remain bound during this transition (2, 59, 63). To test this model, genomic footprinting was used to assess cell cycle-dependent changes in protein-DNA interactions throughout 1.2 kb of DNA that contains both the major and minor *dhfr-rep3* bidirectional promoters.

Detection of protein-DNA interaction at the *dhfr* promoter in vivo. The organization of the *dhfr-rep3* promoter region is shown in Fig. 2. Protein-DNA interactions were examined with a reiterative primer extension assay that permits fine mapping of nuclease cleavage sites relative to known DNA sequences (10). Oligonucleotide primers that anneal to specific sequences within either the top or bottom strands of regions of interest were designed (Fig. 2). Since hamster *dhfr* and *rep3* mRNAs have multiple 5′ ends (14, 45, 46, 49, 64), the positions of primers, promoter elements, and transcript start sites described here are relative to the *dhfr* mRNA ATG translation start site.

CHOC 400 cells were synchronized in early G_1 phase, in mid-G1 phase, at the G_1/S boundary, in early S phase, and in mitosis, as described in Materials and Methods. To prepare footprinting templates, cells attached to tissue culture plates were exposed to buffer containing the permeabilizing agent lysophosphatidylcholine and various concentrations of DNase I for 6 min and then lysed immediately. This rapid footprinting procedure prevented subtle changes in nuclease protection patterns associated with the isolation of nuclei (data not shown). Purified genomic DNA digested with DNase I in vitro was used as the control template. The position of nuclease cleavage sites was determined by comparing the migration of the DNase I digestion products to dideoxy sequencing ladders prepared with the same oligonucleotide primer. Multiple levels of nuclease digestion were used to assess the level of occupancy of protein binding sites (10, 17). For all templates, extension to a restriction endonuclease cleavage site was used to estimate the degree of DNase I digestion in the region of interest. Intermediate levels of digestion were chosen so that approximately 50% of extension products were full length.

The genomic footprint of the major *dhfr* promoter during the cell cycle. Comparisons of the hamster, mouse, and human *dhfr* major promoter sequences reveal several conserved features (reviewed in references 2 and 59) (Fig. 2). Each of these promoter regions contains two overlapping consensus E2F sites oriented in opposite directions near the major transcription start site and a cluster of GC boxes that are homologous to the consensus binding sequence for the transcription factor Sp1 (39). The hamster promoter also contains two rigid DNA regions called SCEs that may reduce the frequency of transcription initiation (54). Using primer 477 (Fig. 3), we first examined the cleavage pattern of the transcribed strand in the proximal *dhfr* promoter region. Compared with the naked-DNA control, the four promoter-proximal GC boxes corresponding to consensus Sp1 binding sites (Sp1 sites 1 through 4) displayed suppression of nuclease cleavage indicative of proteins bound to DNA (Fig. 3, lanes 3 to 12). Footprinting with primer 477 revealed the presence of several DNase I-hypersensitive sites between Sp1 sites 2 and 3 and at the junctions between SCE II and Sp1 site 2 and between SCE I and Sp1 site 1 (Fig. 3, lanes 3 to 12). Cleavage within a fourth putative Sp1 binding site (Sp1 site 4) was also suppressed, although DNase I-hypersensitive sites were not observed at the upstream borders of this site as they were at Sp1 sites 1 through 3 (Fig. 3, lanes 3 to 12).

Although DNase I-hypersensitive sites were observed within SCE I and SCE II near the border of the adjacent Sp1 sites (Fig. 3; compare lanes 3 to 12 with lanes 1 and 2), cleavage at other sites in the SCEs was not suppressed or enhanced compared with that of naked DNA. Thus, the nuclease cleavage patterns are not consistent with the binding of a protein factor

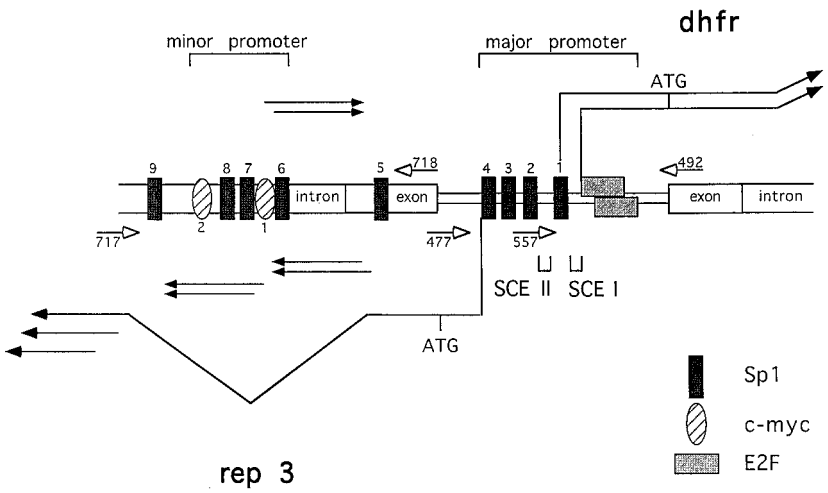

FIG. 2. Organization of the *dhfr* and *rep3* bidirectional promoter region. The major and minor promoter regions for *dhfr* and *rep3* contain nine consensus binding sites for Sp1, two consensus binding sites for c-Myc, two SCEs, and two overlapping binding sites for E2F. Major *dhfr* and *rep3* transcripts are indicated by filled arrows. ATG, the translational start site for *dhfr* mRNA. The locations and orientations of the primers used for genomic footprinting are indicated by open arrows. The first protein-encoding exons for *dhfr* and *rep3* are shown. Note that the minor promoter lies within an intron of a major *rep3* transcript beginning at the major promoter.

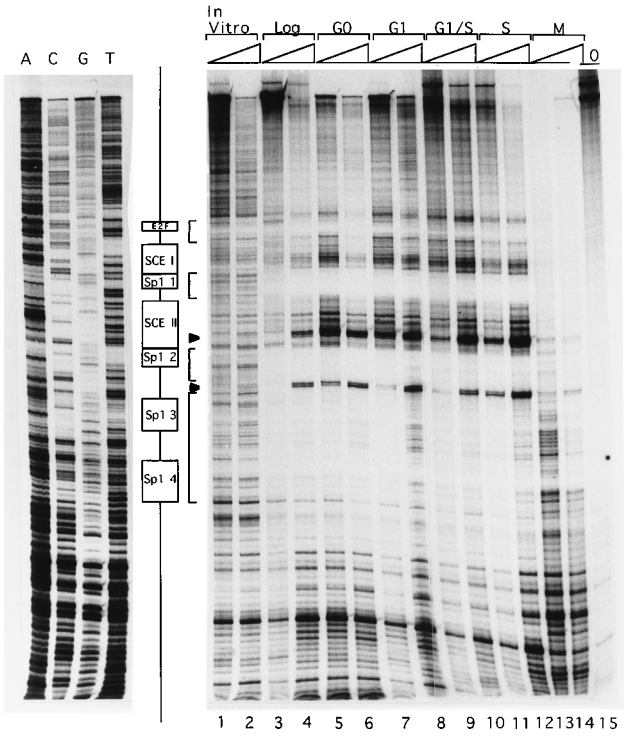

FIG. 3. Genomic footprint analysis of protein-DNA interactions on the transcribed strand of the *dhfr-rep3* major promoter region during the cell cycle. CHOC 400 cells were synchronized at the indicated phase of the cell cycle, as described in Materials and Methods, and then permeabilized in the presence of various concentrations of DNase I. The nuclease cleavage patterns in permeabilized cells at two levels of digestion were compared with those of genomic DNA digested in vitro to an equivalent extent by using reiterative extension of end-labeled primer 477. The positions of nuclease cleavage sites relative to the indicated promoter elements were determined by comparing the migrations of extension products with dideoxy sequencing ladders generated with the same primer (A, C, G, and T [left]). Regions protected from DNase I in permeabilized cells are indicated by brackets. Selected hypersensitive sites discussed in the text are indicated by arrowheads. Lane 15, primer extension products obtained with a DNA template from cells not treated with DNase I (0). M, mitotic cells.

to the SCEs, a result in agreement with previous in vitro studies (54). The nuclease sensitivity of the region encompassing Sp1 sites 1 through 4 corresponds to a zone of DNase I hypersensitivity identified previously by low-resolution techniques (3, 49, 52, 61). The footprints over the cluster of Sp1 sites and SCE I and SCE II showed little variation during the cell cycle; they did not vary markedly as a function of enzyme concentration. These findings indicate that virtually all 1,000 copies of the amplified promoter are bound by protein at Sp1 sites 1 through 4 throughout G_1 and entry into the S phase. The samples from cells in mitosis were overdigested in this experiment (Fig. 3, lanes 13 and 14). Primer extension of genomic DNA cleaved with *Eco*RI but not DNase I showed that background signals from nonspecific polymerase pausing were minimal (Fig. 3, lane 15). Primer 477 also showed that the DNase I cleavage patterns within and beyond the first intron of the *dhfr* gene change during the cell cycle, an issue we will address elsewhere.

Genomic footprinting of the overlapping E2F sites of the major *dhfr* promoter. Although differences between the digestion patterns of permeabilized cells and naked DNA at the E2F site on the transcribed strand are evident in Fig. 3, the location of oligonucleotide primer 477 precludes clear visualization of this cleavage pattern. Therefore, an additional primer (primer 557) was used to view the genomic footprint of the E2F site on the transcribed strand in more detail. Compared with the naked-DNA cleavage pattern (Fig. 4, lanes 1 and 2), the suppression of DNase I cleavage was clearly evident over sequences from −47 to −70 that include the overlapping consensus E2F sites (lanes 2 to 14). The footprint on the transcribed strand included suppression of cleavage at positions −64, −60, −56, and −52 and enhanced levels of cleavage at positions −53, −54, and −57 (Fig. 4). The footprint over this region of the transcribed strand did not vary significantly during the cell cycle, even in cell fractions enriched for cells in mitosis (Fig. 4; compare lanes 1 and 2 with lanes 3 to 14). As with primer 477, primer 557 also showed that the DNase I cleavage pattern of the transcribed portion of the *dhfr* gene (Fig. 4 [vertical arrow]) changed during the cell cycle. Once again, primer 477 provided no evidence of protein binding within SCE I at any time during the cell cycle (Fig. 4 [box]).

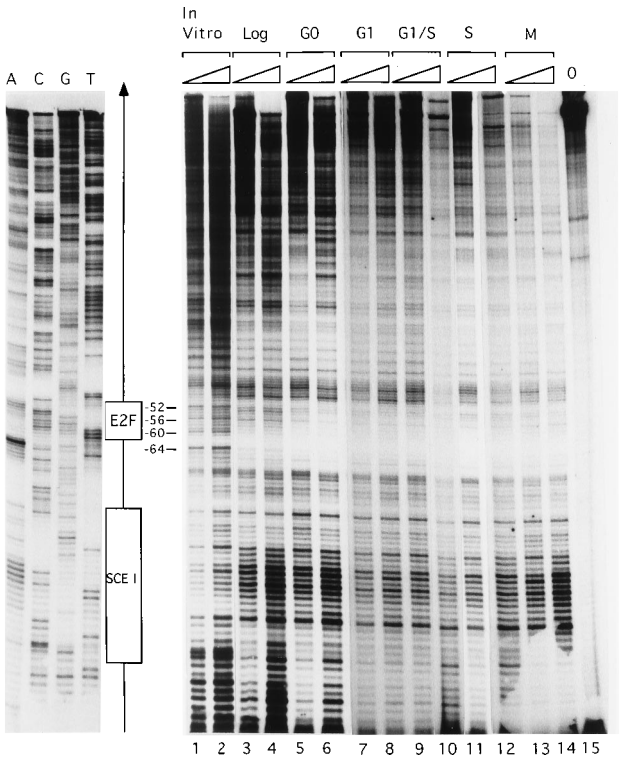

FIG. 4. Genomic footprint analysis of the primary *dhfr* transcription initiation site during the cell cycle. Genomic footprint analysis was performed exactly as described in the legend to Fig. 3 except that the primer extension reactions were performed with primer 557, which detects DNase I cleavages on the transcribed template strand. Specific nucleotide positions within the major *dhfr* transcription initiation site relative to the *dhfr* ATG translational start site are indicated. The vertical arrow indicates the direction of transcription into the *dhfr* gene. Dideoxy sequencing ladders obtained with the same primer (A, C, G, and T) are shown on the left.

The genomic footprint of the major *dhfr* promoter was then examined by using primer 492, which anneals to sequences downstream of the transcription start site and detects nuclease cleavages on the nontranscribed template strand. The suppression of nuclease cleavage in the cluster of Sp1 sites was observed at both levels of DNase I digestion (e.g., Sp1 sites 1 and 2 [Fig. 5]), indicating once again that the vast majority of amplified *dhfr* genes of CHOC 400 cells contain protein factors bound to these sequences. The DNase I cleavage patterns over the Sp1 sites in log-phase cells and in cells collected in G_0/G_1, in mid-G_1, at the G_1/S boundary, and in the S phase were similar (Fig. 5, lanes 3 to 12). In contrast to the cluster of Sp1 sites, the footprint over the E2F sites on the nontranscribed strand changed during the G_1-to-S phase transition. These changes are most evident in comparisons of the frequency of cleavage at position −53 with the protection of Sp1 sites 1 and 2 (Fig. 5). In early G_1 or log-phase cells, the nuclease cleavage pattern of the E2F sites resembled but clearly was not identical to that of naked genomic DNA. For example, minor cleavages at positions −56 and −58 are evident in chromatin but are barely discernible in naked DNA (Fig. 5; compare lanes 1 and 2 with lanes 3 to 6). In permeabilized cells in log phase or G_0/G_1, cleavage at position −53 is evident, as it is in naked DNA (Fig. 5; compare lanes 1 and 2 with lanes 3 to 6). On the opposite strand, these samples also show slightly enhanced cleavage at position −53 (Fig. 4). When cells were induced to traverse G_1 block by the addition of complete culture medium, protection of position −53 at the edge of the E2F site on the nontranscribed strand was observed at multiple levels of digestion (Fig. 5; compare lanes 1 and 2 with lanes 7 and 8). Cleavage at positions −56 and −58, which correspond to conserved residues of the consensus E2F sequence, was strongly suppressed at the lower level of nuclease digestion and also reduced at the higher DNase I concentration. The E2F footprint in cells collected at the G_1/S boundary was identical to that in cells collected at mid-G_1 (Fig. 5; compare lanes 7 and 8 with lanes 9 and 10).

Although the suppression of cleavage within E2F sequences was still evident at higher levels of digestion in samples from both G_1 and G_1/S cells, the cleavage patterns began to resemble those of cells in early G_1 as the level of digestion increased (Fig. 5, lanes 8 and 10). If portions of the E2F sites on the nontranscribed strand of the amplified *dhfr* genes were not occupied by protein factors at these times in the cell cycle, the cleavage pattern would be identical to that of naked DNA at low levels of digestion. The fact that the DNA cleavage pattern began to change at increasing levels of DNase I digestion suggests that even under rapid footprinting conditions, the factors bound at this site were not stable. Note that the region protected from DNase I digestion in G_1 extended beyond the E2F site.

Early in the S phase, the cleavage pattern of the E2F site on the nontranscribed strand was different from that of naked DNA and from that observed in mid-G_1 or at the G_1/S bound-

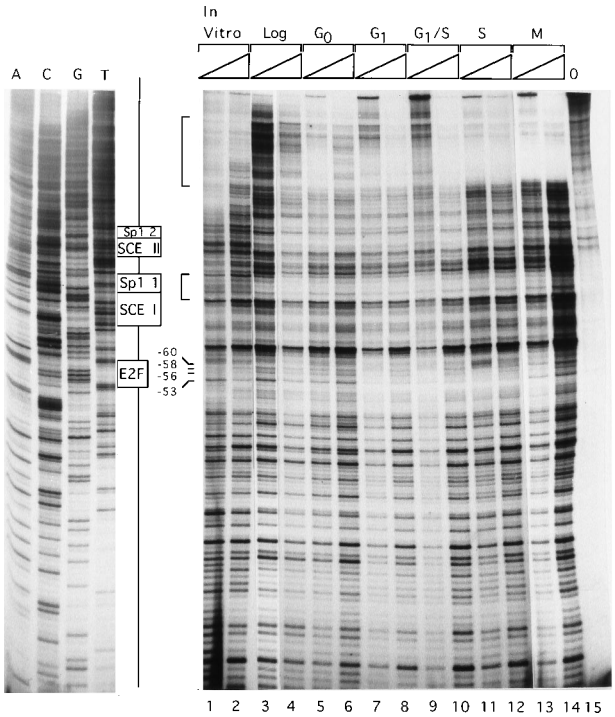

FIG. 5. Cell cycle-dependent interactions of proteins with the E2F site on the nontranscribed strand of the major *dhfr* promoter. Genomic footprint analysis of the E2F site on the nontranscribed strand was performed during the cell cycle as described in the legend to Fig. 3 except that the primer extension reactions were performed with primer 492. Specific nucleotide positions relative to the *dhfr* ATG translational start site are indicated. Boxes denote elements of the major promoter located within the resolved portion of the gel. Dideoxy sequencing ladders obtained with the same primer (A, C, G, and T) are shown on the left. The small bracket indicates the protection of Sp1 site 1, as discussed in the text. The large bracket indicates the protection from DNase I digestion due to protein-DNA interactions at the minor promoter.

ary (Fig. 5; compare lanes 7 to 10 with lanes 11 and 12). At low levels of digestion, a cluster of three hypersensitive bands corresponding to cleavage at the upstream edge of the E2F site at nucleotide positions −59, −60, and −61 was observed (Fig. 5, lane 11). Subtle changes in the cleavage pattern at these sites were also evident at higher levels of digestion (Fig. 5, lane 12). Interestingly, these DNase I-hypersensitive sites map adjacent to the −63 transcription start site responsible for 85% of *dhfr* transcripts (14, 45, 46, 49). However, these signals did not arise from reverse transcription of *dhfr* mRNA by *Taq* polymerase since they were not observed at earlier times in the cell cycle when *dhfr* mRNA was plentiful nor were they observed with templates from cells not treated with DNase I (Fig. 4, lane 15). Primer 492 also revealed a large protected region upstream of the major *dhfr* promoter (Fig. 5). Further analysis shows that this large footprint is due to protein-DNA interactions within two upstream regions, the first *rep3* intron and the minor promoter discussed below.

Together with footprints from the transcribed strand, these results indicate that each copy of the amplified *dhfr* gene is bound during all of G_1 and the early S phase by a transcription complex that includes proteins bound both at Sp1 sites 1 through 4 and at sequences which include the overlapping E2F sites at the major *dhfr* transcription initiation site. Changes in the DNase I cleavage patterns at the boundaries of SCE I and SCE II suggest that these SCEs are structurally distorted by the formation of this transcription complex. While a number of protein-DNA interactions associated with the basal transcription complex did not vary significantly during the transition of G_1 and entry into the S phase, the nuclease digestion patterns of the overlapping E2F sites on the nontranscribed strand did change during the G_1-to-S phase transition and during the S phase. The cleavage patterns on the transcribed and nontranscribed strands were reproducible in three cell cycle experiments in which the same DNA templates were used for extension reactions with primers 492 and 477.

The major *dhfr* initiation site binds multiple protein factors. Genomic footprinting provided evidence of protein contacts over a 30-bp region of the major *dhfr* transcription initiation site in CHOC 400 cells (Fig. 4 and 5). Sequence comparisons show that an 18-bp segment of the genomic footprint which includes two overlapping E2F sites is highly conserved in the mouse, human, and hamster promoters (49) (Fig. 6A). To detect changes in protein binding to the overlapping E2F sites during the cell cycle, a double-stranded DNA probe spanning 30 bp of the genomic footprint region was prepared (2-site probe [Fig. 6B]) and incubated with extracts from synchronized and log-phase cells. To ascertain the specificity of E2F protein interactions with the native transcription initiation site, three oligonucleotide competitors were prepared (Fig. 6B). The CG competitor contains the same sequence as one of the *dhfr* E2F sites (i.e., TTT**CG**CGC) but contains flanking sequences that differ from those of the major *dhfr* promoter. Similarly, the GG competitor contains the sequence of the second *dhfr* E2F site (i.e., TTT**GG**CGC), along with the same flanking sequences as those of the CG probe. The third competitor contains the native initiation site with a single G-to-T nucleotide change in the overlapping E2F sites. As a control for E2F gel mobility shift experiments, we examined Sp1 and Oct1 binding in the same whole-cell extracts (Fig. 7A and B). Gel mobility shift experiments were performed with both equal amounts of protein and equal amounts of extracts from an equivalent number of cells. Since the results were essentially identical, the results of experiments with equal amounts of extract are presented here.

Sp1 DNA binding activity was observed as two bands, both

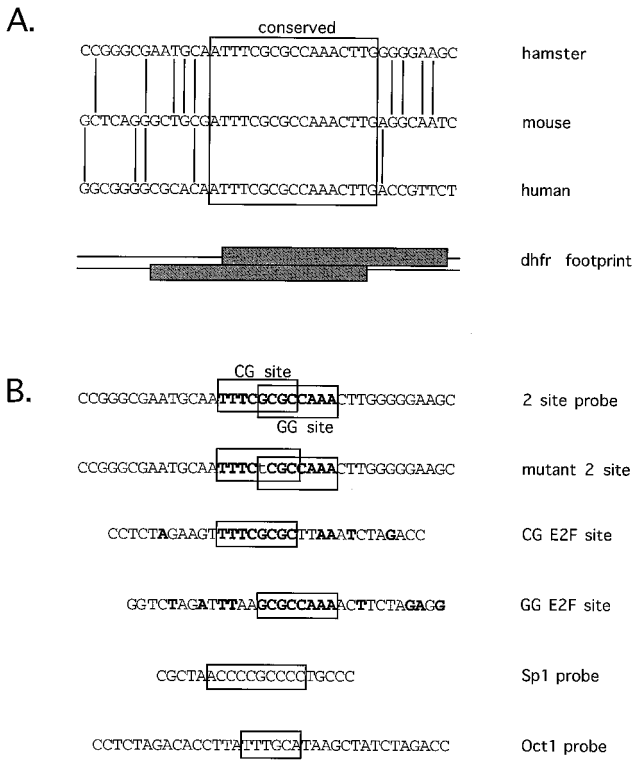

FIG. 6. Sequences at the overlapping E2F sites of the *dhfr* promoter. (A) Comparison of the promoter sequences from hamsters, mice, and humans. A highly conserved 18-bp segment of the major *dhfr* promoter containing two overlapping E2F sites is encompassed by the genomic footprint observed in CHOC 400 cells. Nucleotide residues shared by mouse, human, and hamster sequences flanking the conserved region are indicated by vertical lines. (B) DNA probes for gel mobility shift analysis. Double-stranded DNA oligonucleotides representing the native *dhfr* transcription initiation site (2-site probe), the initiation site with a single G-to-T change in the overlapping E2F sites (mutant 2 site), a single E2F site with the sequence TTTCGCGC (CG E2F site), a single E2F site with the sequence TTTGGCGC (GG E2F site), a consensus Sp1 binding site, and a consensus Oct1 binding site were prepared. The nucleotides in E2F consensus sequences and the residues of single-site probes that match those in the same positions in native *dhfr* E2F flanking sequences are in boldface type.

of which were inhibited by unlabeled Sp1 probe (Fig. 7A, lane 8) but not by the E2F CG, GG, or 2-site probe (lanes 9 and 10) (data not shown). Sp1 binding in extracts from cells in G_0/G_1, early G_1, or S phase did not vary significantly from that in extracts from log-phase cells (Fig. 7A; compare lane 2 with lanes 3, 4, and 6). Sp1 binding was elevated in cells synchronized at the G_1/S boundary with mimosine (Fig. 7A, lane 5) and was reduced in cells in mitosis (lane 7). Fluctuations in the DNA binding activity of Sp1 did not appear to correlate well with the accumulation of *dhfr* mRNA during the G_1-to-S phase transition. As a control, the DNA binding activity of Oct1, which is not known to interact with the *dhfr* promoter, was also examined. As with Sp1, Oct1 DNA binding activity varied little during the G_1-to-S phase transition of the cell cycle (Fig. 7B).

In contrast to Sp1 and Oct1, protein binding to the major *dhfr* transcription initiation site fluctuated during the cell cycle (Fig. 7C). As discussed below, at least five specific protein-DNA complexes are observed in hamster cell extracts when the native initiation site (or 2 site) is used as the probe. We refer to these protein-DNA complexes as complexes A through E. In comparison to extracts from log-phase cells, extracts from G_0/G_1 and early-G_1 cells contained reduced initiator site bind-

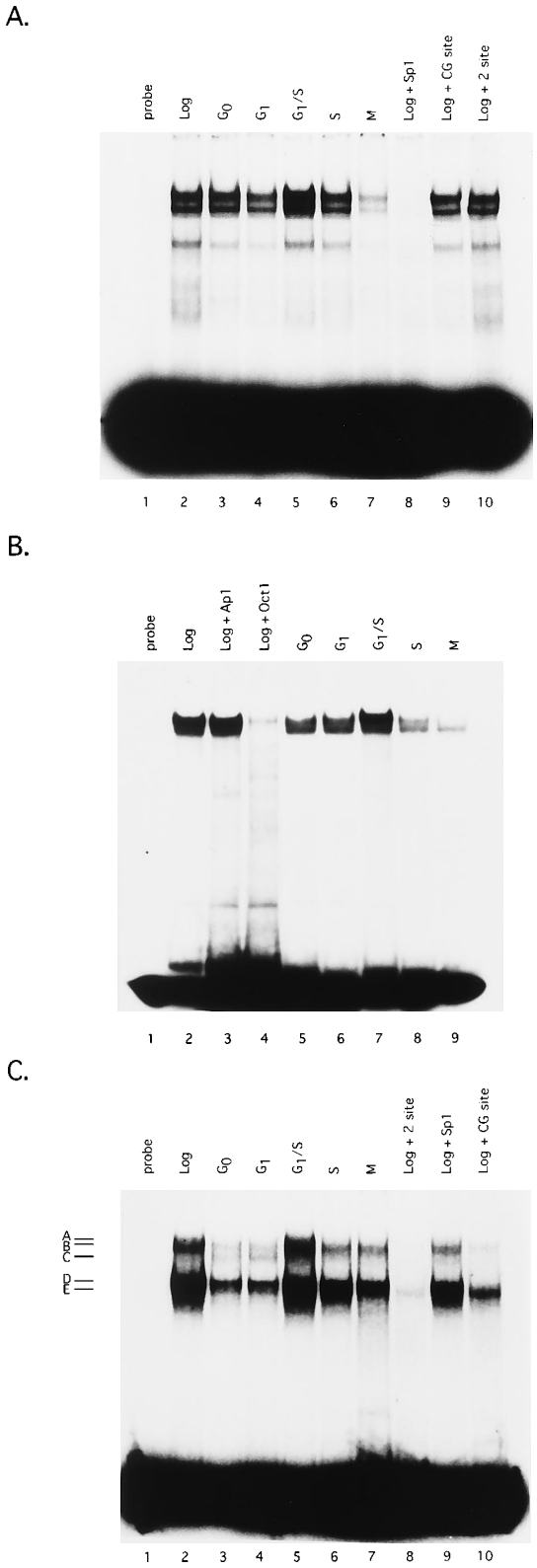

FIG. 7. Comparison of Sp1, Oct1, and *dhfr* initiation site DNA binding activities during the cell cycle. Equivalent amounts of whole-cell extracts from synchronized and log-phase cells were incubated with labeled double-stranded DNA probes, resolved by neutral polyacrylamide electrophoresis, and visualized by autoradiography. (A) Sp1 DNA binding activity during the cell cycle. Lane 1, probe alone; lanes 2 to 7, Sp1 DNA binding activities in the indicated cell cycle extracts; lanes 8 to 10, log-phase extract with unlabeled Sp1 (lane 8), E2F CG site (lane 9), or E2F 2-site (lane 10) probe as a competitor. (B) Oct1 DNA binding activity during the cell cycle. Lane 1, probe alone; lanes 2 to 4, log-phase extract with no competitor (lane 2) or with unlabeled AP1 (lane 3) or Oct1 (lane 4) probe as a competitor; lanes 5 to 9, Oct1 DNA binding activities in the indicated cell cycle extracts. (C) Protein-DNA complexes formed on the 2-site E2F probe during the cell cycle. Lane 1, probe alone; lanes 2 to 7, 2-site E2F DNA binding activities in the indicated cell cycle extracts; lanes 8 to 10, log-phase extract with unlabeled 2-site (lane 8), Sp1 (lane 9), or CG E2F site (lane 10) probe as a competitor. The positions of protein-DNA complexes A through E, discussed in the text, are indicated on the left. M, mitotic cells.

ing activity (Fig. 7C; compare lane 2 with lanes 3 and 4). Note that extracts from G_0/G_1 and G_1 cells displayed elevated amounts of binding complex C (Fig. 7C, lanes 3 and 4). In log-phase cells, cells synchronized at G_1/S with mimosine, and early-S-phase cells, complex E was evident (Fig. 7C, lanes 5 and 6). Binding activity was also evident in cell fractions enriched for cells in mitosis (Fig. 7C, lane 7). Thus, in contrast to Sp1, the DNA binding activities that recognize the primary *dhfr* transcription initiation site varied during the cell cycle. In this experiment, competition with the single CG E2F site showed that the 2-site probe binds a protein factor that does not recognize the TTTCGCGC sequence (Fig. 7C, lane 10).

To examine the specificity of protein interactions with the native initiation site further, protein extracts from unsynchronized cells in log-phase growth were incubated with the 2-site probe in the presence of several competitors (Fig. 8A). This experiment confirmed that complex E is not inhibited by the CG competitor (Fig. 8A, lane 4) and showed that the mutant 2-site probe competes for complex E but not for complexes A through D (Fig. 7C, lane 7). Together, these data indicate that all of the factors responsible for the formation of complexes on the 2-site probe do not bind the CG E2F single-site competitor with high affinity. We then compared protein binding to the CG and GG single-E2F-site probes during the cell cycle (Fig. 8B and C). The protein binding patterns of the CG single-E2F-site probe varied during the cell cycle in a manner quite similar to that of the 2-site probe (compare Fig. 8B with Fig. 7C). Compared with the binding activity in extracts from cells in log phase, binding was lower in extracts from cells in G_0/G_1, early G_1, or S phase, particularly in complexes A and B (Fig. 8B; compare lane 2 with lanes 3, 4, and 8). Binding activity in complexes A and B was elevated in extracts from cells synchronized at the G_1/S boundary (Fig. 8B, lanes 5 and 6) and diminished in cells collected in mitosis (lane 11).

A very different pattern of protein binding to the GG single-E2F-site probe was observed during the cell cycle (Fig. 8C). Protein binding in extracts from cells in log, G_0/G_1, early G_1, G_1/S, or S phase or from mitotic cells showed little fluctuation (Fig. 8C, lanes 2 to 7), except that elevated levels of complex C were observed in G_0 and G_1 samples (lanes 3 and 4). In marked contrast to the CG single-site probe, the levels of the factors that bind the GG single-E2F-site probe were not markedly elevated in cells synchronized at the G_1/S boundary with mimosine (Fig. 8C, lane 5), nor were they reduced as significantly as those of the factors that bind the CG probe in mitotic cells (compare Fig. 8C, lane 7, with Fig. 8B, lane 11). As with the GG single-site probe, the 2-site probe retained significant binding activity in mitosis (Fig. 7C, lane 7). Thus, the CG and GG sites within the major *dhfr* promoter bind distinct species of E2F (68b).

The genomic footprint of the minor *dhfr-rep3* promoter region. In transient-transfection studies, the upstream cluster of Sp1 sites beyond −200 in the major *dhfr* promoter region has little effect on *dhfr* transcription (45, 60, 64). Instead, these sequences regulate the transcription of a class of *rep3* tran-

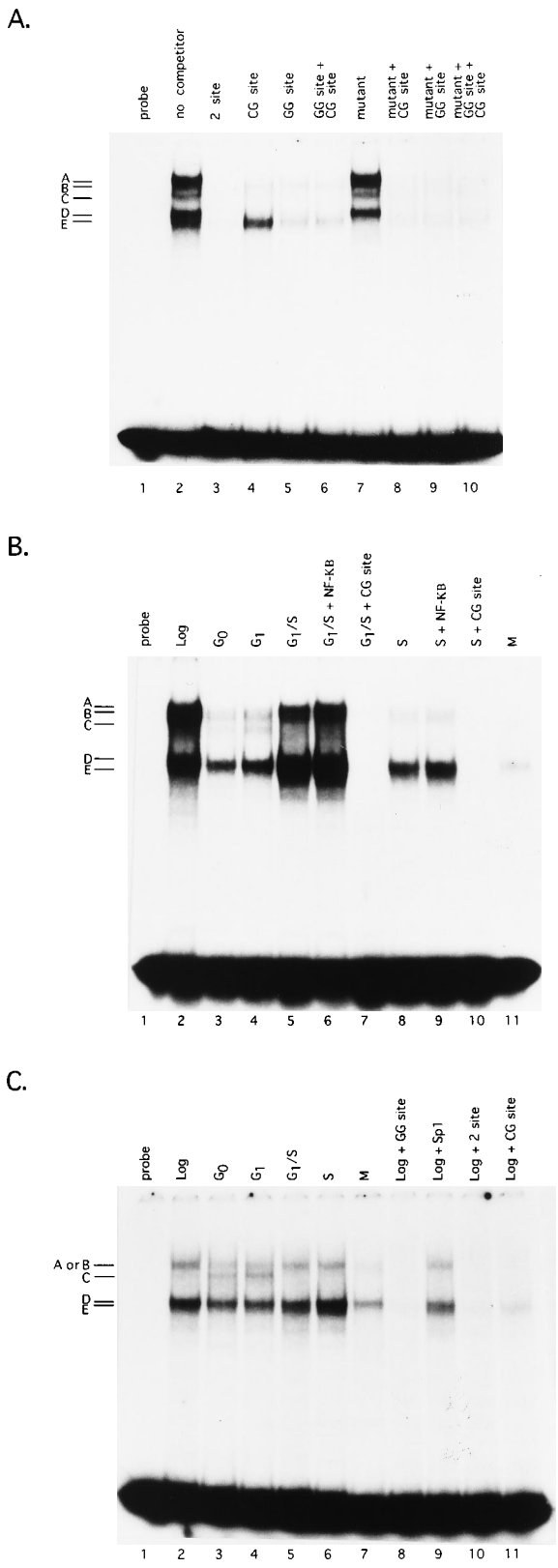

FIG. 8. The TTTCGCGC and TTTGGCGC E2F sites bind different factors during the cell cycle. Equivalent amounts of whole-cell extracts from synchronized and log-phase cells were assayed for DNA binding activities as described in the legend to Fig. 7. (A) Log-phase extracts were incubated with the 2-site probe plus the indicated unlabeled competitors. The positions of protein-DNA complexes A through E are indicated on the left. (B) CG E2F site DNA binding activity during the cell cycle. Lane 1, CG E2F site probe alone; lanes 2 to 5, 8, and 11, CG E2F site probe plus the indicated log-phase or cell cycle extract; lanes 6 and 7, CG E2F site probe plus G_1/S-phase extract with unlabeled NF-κB (lane 6) or CG E2F site (lane 7) as a competitor; lanes 9 and 10, CG E2F site probe with S-phase extract plus unlabeled NF-κB (lane 9) or CG E2F site (lane 10) as a competitor. (C) CG E2F site DNA binding activity during the cell cycle. Lane 1, GG E2F site probe alone; lanes 2 to 7, GG E2F site probe plus the indicated cell cycle extract; lanes 8 to 11, GG E2F site probe plus log-phase extract with unlabeled GG E2F site (lane 8), Sp1 (lane 9), 2-site (lane 10), or CG E2F site (lane 11) probe as a competitor.

scripts that lack a conserved exon located between the major and minor promoters (45, 49, 60). To better understand the relationship between the major and minor promoters in gene expression, we examined protein-DNA interactions throughout a 500-bp region that includes the minor *rep3* promoter. With primer 718, several prominent footprints were evident in this region; the most obvious occurred over an 85-bp GC-rich region from −480 to −564 containing three matches to the Sp1 consensus sequence (56) and two matches to the c-Myc E-box binding site consensus sequence (CACGTG) (reference 57 and references therein). As shown in Fig. 9, primer 718 revealed suppression of DNase I cleavage at multiple levels of digestion throughout the sequences encompassing Sp1 sites 6, 7, and 8 and the putative c-Myc binding site (c-Myc site 1; CACCTG) located between Sp1 sites 6 and 7 (Fig. 9; compare lanes 1 and 2 with lanes 3 to 12). A second putative c-Myc binding site (CACGTG) at positions −555 to −561 (designated c-Myc site 2) was protected from cleavage at both levels of digestion throughout the G_1 and S phases (Fig. 9, lanes 3 to 12). Several DNase I-hypersensitive sites were also evident in this region; a prominent hypersensitive site was observed at the upstream edge of c-Myc site 2, and a cluster of hypersensitive bands was observed between this site and Sp1 site 8 (Fig. 9 [arrowheads]). The protection of this cluster of Sp1 sites was reduced in cell fractions enriched for mitotic cells (Fig. 9; compare lanes 3 to 12 with lanes 13 and 14). With primer 718, a large footprint over the region from −408 to −445 was also observed.

Similar results were obtained when the nuclease protection patterns on the opposite strand with primer 717 were viewed (Fig. 10). Both protection from nuclease cleavage and the induction of hypersensitive sites indicate that proteins were bound to Sp1 sites 6, 7, and 8, which encompass c-Myc site 1. Because Sp1 sites 6 and 7 directly abut the six-base consensus sequence of c-Myc site 1, it is not possible to ascertain whether the genomic footprint reflects the binding of c-Myc or related proteins at c-Myc site 1. The suppression of nuclease cleavage at c-Myc site 2 was readily apparent at all times in the G_1-to-S transition (Fig. 10, lanes 3 to 12). While some differences in the footprints over the c-Myc and Sp1 sequences at the minor promoter were observed early in the cell cycle, these differences appeared to be related more to quantitative changes in the intensity of the signal than to qualitative changes in the digestion pattern (e.g., compare lane 4 with lane 9 in Fig. 10). Thus, the nuclease protection patterns of the minor promoter region suggest that Sp1 and proteins which recognize c-Myc site 2 are responsible for establishing a transcription complex that persists throughout most of the cell cycle.

Our footprinting assay is sufficiently sensitive to detect subtle changes in protein-DNA interactions at known promoter elements during traversal of the cell cycle. Under these conditions, no footprints are observed within the first exon of the *dhfr* gene or in the conserved *rep3* exon located between the major and minor promoters (Fig. 4, 9, and 10). However, both

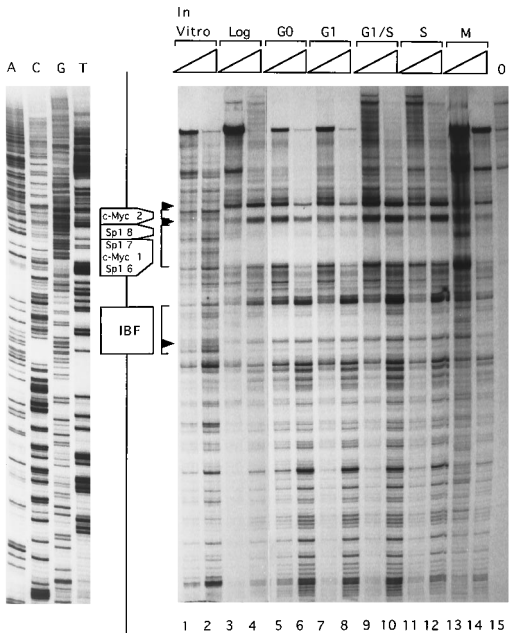

FIG. 9. Protein-DNA interactions on the nontranscribed strand of the minor promoter region during the cell cycle. Genomic footprint analysis was performed as described in the legend to Fig. 3 except that the primer extension reactions were conducted with primer 718. Binding sites for Sp1, c-Myc, and rep3 IBF are indicated by open boxes. Regions protected from DNase I cleavage in permeabilized cells are indicated by brackets. Arrowheads denote major DNase I-hypersensitive sites in permeabilized cells. Dideoxy sequencing ladders generated with the same primer (A, C, G, and T) are shown on the left. Lane 15, extension products from DNA templates not treated with DNase I (0). M, mitotic cells.

primer 718 and primer 717 reveal the presence of a large footprint at positions −408 to −445 (Fig. 9 and 10). This footprint is due to a novel DNA binding activity that recognizes a 36-bp sequence near the border between the first exon and the first intron of the primary *rep3* transcript. We have named this factor the rep3 intron binding factor (IBF). Neither rep3 IBF nor its binding site has been implicated in the regulation of transcription initiation; its role in gene expression is presently unknown.

The genomic footprint of the *dhfr-rep3* promoter region in mitotic cells. To determine if protein factors are bound to the *dhfr-rep3* promoter region in mitotic chromosomes, our footprinting experiments included nonadherent cells isolated from cultures which had been treated with Colcemid for 2 to 4 h. In contrast to our other cell fractions, which contained up to 85% of the cells poised at a specific interval in the cell cycle, approximately 50% of the cells in our mitotic cell fractions were nonadherent cells in late S phase or other parts of the cell cycle (data not shown). Nonetheless, footprinting templates were prepared from these cell fractions and examined by using the same primers and extension conditions as before (Fig. 3 to 5, 9, and 10). While in some instances we clearly observed the loss of DNase I protection in this cell fraction (e.g., at the E2F site [Fig. 4] and the Sp1 and c-Myc sites [Fig. 9]), in other instances the cleavage pattern was not perceptibly changed. In particular, we have never observed the prominent footprint on the transcribed strand at the primary transcription start site of the major *dhfr* promoter to be diminished in any cell fraction (Fig. 4, lanes 13 and 14).

DISCUSSION

The regulation of eucaryotic gene expression occurs through the interplay of multiple transcription factors. Here we have used genomic footprinting to survey a region of DNA containing the promoters and 5′ ends of two genes for protein-DNA interactions that may be important for regulating the initiation of transcription during the cell cycle. Our footprinting results, which are summarized in Fig. 11, identify protein-DNA interactions throughout 1.2 kb of DNA encompassing both the *dhfr* and *rep3* major and minor promoters. With the exception of a prominent protein-DNA interaction within the first intron of the *rep3* gene, all the protein-DNA interactions within this region mapped to sequences known to be important for the regulation of transcription (reviewed in reference 59). The only changes in protein-DNA interactions detected during the cell cycle occurred at the overlapping E2F sites at the major *dhfr* promoter, and only the changes in the digestion pattern on the nontranscribed template strand appeared to correlate with the accumulation of *dhfr* mRNA during the G_1-to-S phase transition. Although *rep3* mRNA levels fluctuated slightly during the cell cycle, our results suggest that *rep3* transcription is not coordinately regulated with *dhfr* transcription in CHO cells.

Transcription initiation complexes at the major *dhfr-rep3* promoter. The assembly of transcription initiation complexes at classical polymerase II (Pol II) promoters in vitro begins with the binding of TFIID to the TATA box (reviewed in reference 71), a regulatory element located approximately 30 bp upstream of the transcription start site. The binding of TFIID precipitates a series of ordered protein-DNA and protein-protein interactions that leads to initiation complexes which support basal levels of transcription. The modulation of

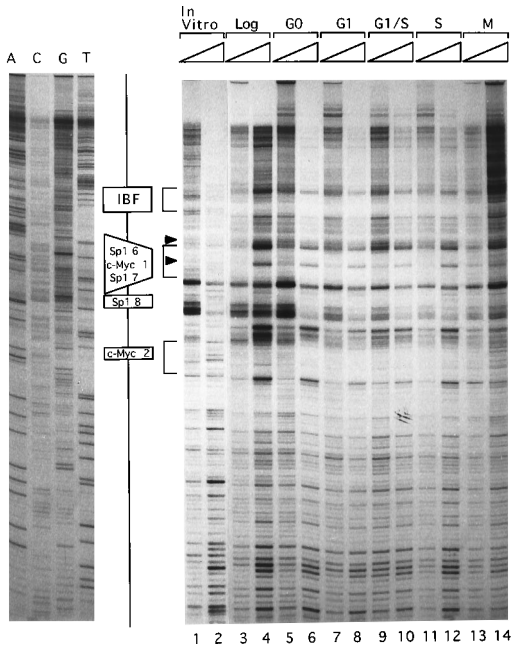

FIG. 10. Protein-DNA interactions on the transcribed strand of the minor promoter region during the cell cycle. Genomic footprint analysis of cells in exponential growth (Log) or synchronized at the indicated phase of the cell cycle was performed as described in the legend to Fig. 3 except that the primer extension reactions were performed with primer 717. Open boxes denote the positions of Sp1, c-Myc, and rep3 IBF binding sites. Regions protected from DNase I cleavage are indicated by brackets; two major DNase I-hypersensitive sites are indicated by arrowheads.

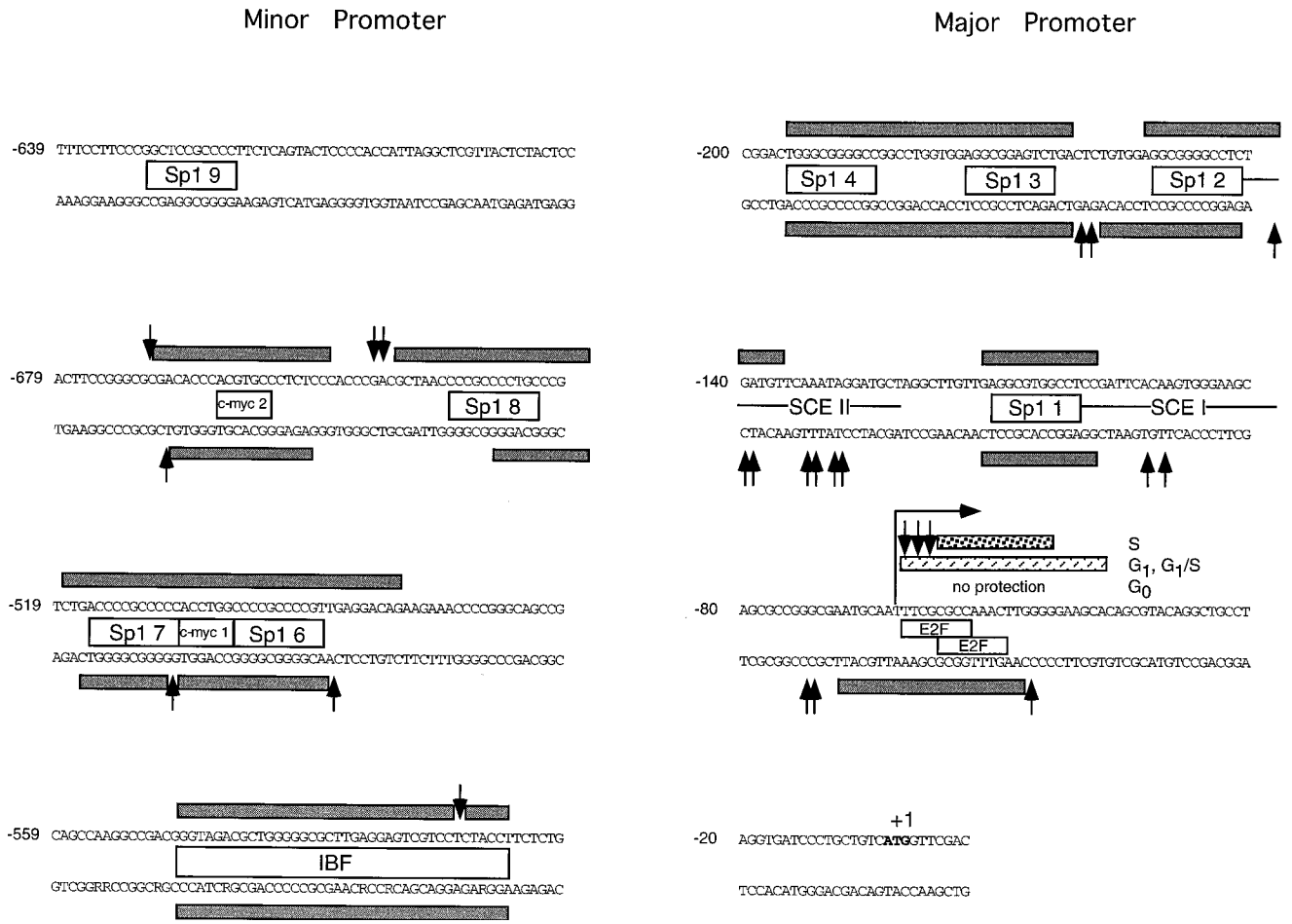

FIG. 11. Summary of protein-DNA interactions throughout the major and minor promoters during the cell cycle. The regions of the major and minor promoters protected from DNase I cleavage in permeabilized CHOC 400 cells (Fig. 3 to 5, 9, and 10 and data not shown) relative to the promoter DNA sequence on each template strand are indicated by shaded boxes. Open boxes denote binding sites for Sp1, c-Myc, rep3 IBF, and E2F. Major DNase I-hypersensitive sites are indicated by vertical arrows. The primary *dhfr* transcription initiation site is indicated by a right-angled arrow. Cell cycle-dependent variations in the cleavage patterns over the E2F site on the nontranscribed strand are indicated. Nucleotide positions are numbered relative to the *dhfr* ATG translational start site. No footprints were observed between −200 and −400 or within the first exon of the *dhfr* gene.

transcription initiation is then achieved by *trans*-acting regulatory transcription factors that bind DNA or by other proteins that associate with factors within the transcription complex. In contrast to classical Pol II promoters, a subset of mammalian genes, including *dhfr*, contains no obvious TATA box (reviewed in reference 2). Nonetheless, TFIID is required for transcription from these promoters (2, 56). From the results of in vitro DNase I footprinting experiments with purified TATA-binding protein (TBP), the DNA binding component of TFIID, Wiley et al. have suggested that TBP binds to conserved sequences located in SCE I of the human *dhfr* promoter (69). Since the sequences protected by TBP in vitro are not protected from nuclease cleavage on either strand in permeabilized CHOC 400 cells and a CAA triplet within the putative TBP binding site is not required for *dhfr* promoter activity (12), we conclude that TBP does not bind to the −30 region of the *dhfr* promoter in cells. In addition, genomic footprinting provides no evidence of TBP binding at the minor promoter. Presumably, TBP is recruited to the *rep3-dhfr* major and minor promoters by interactions with other transcription factors bound to DNA, as described below.

At the major *dhfr* promoter, genomic footprinting indicates that proteins are bound to a cluster of Sp1 sites (Sp1 sites 1 through 4) and the primary *dhfr* transcription initiation site throughout most of the cell cycle. Since this complex of proteins is observed in early G_1 when *dhfr* transcription is low, these protein-DNA interactions likely reflect an initiation complex that supports basal levels of transcription. This complex may also be responsible for suppressing *dhfr* transcription in quiescent cells. Although other transcription factors are able to bind consensus Sp1 sites (reviewed in reference 2), the protection observed at the major *dhfr* promoter is likely due to Sp1 for the following reasons: Sp1 has been shown to activate transcription from the *dhfr* promoter in cells (66), point mutations in the *dhfr* promoter that interrupt Sp1 binding in vitro severely reduce *dhfr* transcription in transient-transfection assays (12), and Sp1 often acts through clusters of binding sites (1, 11). Indeed, we have never observed the protection of two isolated consensus Sp1 binding sites (sites 5 and 9) from DNase I cleavage at any time in the cell cycle (Fig. 4, 9, and 10; also data not shown). Both genomic footprinting and gel mobility shift analysis of Sp1 binding in vitro indicate that alterations in Sp1 DNA binding activity are not responsible for growth-dependent changes in *dhfr* gene expression. However, our results do not preclude the possibility that posttransla-

tional modifications of Sp1 bound to DNA contribute to cell cycle regulation of *dhfr* transcription.

E2F and the regulation of *dhfr* transcription. Our studies of protein-DNA interactions with the two overlapping E2F sites at the primary *dhfr* transcription initiation site indicate that these sites serve different functions in *dhfr* gene regulation. First, we observe subtle differences between the genomic footprints on the transcribed and nontranscribed template strands of the overlapping E2F sites. Since these differences are reproducibly observed with different primers on the same DNA templates, they likely reflect important features in the organization of the *dhfr* transcription initiation complex in the cell. As shown in the summary of the footprinting data in Fig. 11, the DNase I footprints on the transcribed and nontranscribed strands are markedly asymmetrical with regard to the position of the overlapping E2F sites. Since the overlapping E2F sites are inverted relative to one another, the asymmetry of the footprints may reflect the orientation of E2F complexes bound to DNA in opposite orientations.

On the transcribed strand, protection from cleavage is observed at nucleotide positions −47 to −70 throughout the cell cycle (Fig. 4). The protected sequences extend beyond the highly conserved central 18 bp of the overlapping E2F sites located at nucleotide positions −51 to −62. Although there are few strong DNase I cleavage sites on the opposite strand within this region, the cleavage patterns on the opposite strand differ from those of naked DNA (Fig. 5), suggesting that the protein constitutively bound at the transcription initiation site contacts both DNA strands. Perhaps the protein constitutively bound at the *dhfr* transcription initiation site produces a DNA conformation that positions the CG E2F site for the subsequent binding of cell cycle-regulated E2F complexes. In G_0/G_1, sequences over the upstream CG E2F site on the nontranscribed strand are susceptible to DNase I cleavage, particularly at position −53 (Fig. 5). When protected from digestion in G_1, DNase I cleavages on the nontranscribed strand are also suppressed within and beyond the central conserved 18 bp of the overlapping E2F sites (Fig. 5 and 11). Thus, from our footprinting results we suggest that at least two protein factors bind to the primary *dhfr* transcription initiation site; one is constitutively bound at all times during the cell cycle, while the second is recruited to the overlapping E2F sites during transition through G_1.

The notion that the *dhfr* transcription initiation site is recognized by two distinct species of E2F is reinforced by examination of protein binding to the overlapping E2F sites by gel mobility shift assays. The results of experiments presented in Fig. 7 and 8 clearly show that the hamster proteins which recognize the TTTGGCGC E2F single-site probe are not identical to those which recognize the TTTCGCGC E2F single-site probe. For example, the data in Fig. 8A show that the binding activity of complex E formed on the 2 site probe is not inhibited by TTTCGCGC but is inhibited by TTTGGCGC (compare lanes 4 and 5). The mutant 2-site competitor is unable to compete for complexes A through D but does disrupt complex E (Fig. 8A, lane 7). Since the mutant 2-site probe alters both E2F sites, this result shows that only complex E is able to form on the mutant 2-site probe. However, comparisons of protein binding to the CG and GG probes during the cell cycle also show that clearly these two sequences are recognized by distinct factors. The CG E2F binding activity fluctuates during the cell cycle (Fig. 8B), while the GG E2F binding activity does not (Fig. 8C). Thus, the GG binding activity may represent the factor responsible for the constitutive footprint observed throughout the cell cycle at the primary *dhfr* transcription initiation site, and the CG binding activity may represent the activity that protects the E2F sequences on the nontranscribed strand during the G_1-to-S phase transition.

Our results present several important questions concerning the roles of the overlapping E2F sites in the regulation of *dhfr* transcription. A recent report has suggested that the overlapping E2F sites at the *dhfr* promoter function by increasing the half-lives of E2F-DNA complexes from seconds to minutes (67). Our results are inconsistent with this interpretation; the CG single-site competitor is unable to diminish the interaction of one species of E2F with the GG single-site probe in a 20-min binding reaction in vitro (Fig. 7 and 8). Instead, we conclude that the overlapping E2F sites bind at least two distinct species of E2F. One important issue that remains to be addressed is whether two distinct species of E2F can simultaneously bind the overlapping E2F sites. On the basis of the inverted organization of the E2F sequences and the asymmetry of the genomic footprints, it is possible that the two distinct species of E2F are oriented in opposite directions on the face of the DNA helix. If so, a species of E2F bound at the TTTGGCGC site early in the cell cycle may provide a protein-DNA complex that discriminates between other species of E2F appearing later in the cell cycle. Differential binding of different E2F species to overlapping and inverted sites may help explain the ability of these sites both to repress basal transcription and to mediate growth-dependent induction of gene expression (37). Finally, our results also resemble those obtained with the human *p107* promoter in that a TTTGGCGC E2F site at the transcription initiation site is critical for basal promoter activity, while an upstream TTTCGCGC E2F site is required for the suppression of transcription by pRb or p107 (72). Although a protein, called HIP1, that binds sequences at the initiation site of the mouse *dhfr* promoter was reported (47), this activity was later attributed to E2F-1 (63).

We are interested in the identification of the two or more species of E2F that participate in the regulation of *dhfr* gene expression. Recent work shows that biologically relevant forms of E2F are heterodimeric complexes composed of one E2F polypeptide and one DP polypeptide that act synergistically to activate transcription from E2F DNA binding sites (4, 33, 35). (Here we refer to E2F as the collection of heterodimeric transcription factors and to E2F-1, E2F-2, etc., as specific subunits of E2F.) To date, cDNA clones have been reported for mammalian E2F-1 (32, 40), E2F-2 (36, 44), E2F-3 (44), E2F-4 (5, 27), E2F-5 (27), DP-1 (29), and DP-2 (28, 70). The specific roles of individual E2F and DP proteins in gene expression are not well understood. E2F-DP complexes interact with important cell cycle regulators, including pRb, p107, p130, and cyclin A/cdk2, and these regulators have been shown to modulate the transactivation activity of E2F in vitro and in cells during the G_1-to-S phase transition (8, 9, 13, 19, 32, 40, 41, 44). Heterodimers composed of various E2F and DP family members have different abilities to form complexes with the retinoblastoma (pRb) family of cell cycle regulators (13, 16, 20, 27, 43) and various abilities to transactivate reporter genes from consensus E2F binding sites (27, 33, 44). E2F and DP subunits also show differences in expression among tissues and at different times in the cell cycle (27, 44, 70).

On the basis of work by others showing that E2F complexes with slower mobilities (e.g., complexes A, B, and C [Fig. 7]) contain cell cycle-regulatory proteins, such as pRb, p107, p130, and cyclin-dependent (cdk) protein kinase complexes (8, 9, 13, 16, 20, 41, 44, 50, 68), we have begun examining the constituents of complexes A through E that are formed on the *dhfr* transcription initiation site. By using both antibodies to specific factors and protein expression experiments with CHOC 400 cells, our data indicate that E2F-2 and E2F-4 are the primary

E2F species regulating *dhfr* gene expression (68a). Although increases in E2F-1 mRNA correlate with the induction of *dhfr* transcription in mouse cells (63), the expression of E2F-1 in quiescent rat REF52 cells has a minimal effect on *dhfr* gene expression (15) and the expression of E2F-1 does not induce *dhfr* transcription in CHOC 400 cells (68b).

While increases in TTTCGCGC DNA binding activity show a general correlation with the induction of *dhfr* gene transcription, at present we are not able to directly correlate the appearance of a specific gel mobility shift protein complex with features of the genomic footprints and *dhfr* gene transcription. For example, during the transition of G_1, E2F sites on the nontranscribed template strand at the primary *dhfr* transcription initiation site become protected from DNase I digestion. On the 2-site probe, both complexes A and B are present in small amounts in early G_1 and mid-G_1 (Fig. 7C, lanes 3 and 4) and reach maximal levels at the G_1/S boundary (lanes 5 and 6) prior to declining in the S phase (lanes 8 and 9). Complex C also accumulates during the transition of G_1 and then declines in S phase (Fig. 5A, lanes 3 to 8). Similarly, complex E is most prevalent at the G_1/S boundary and in early S phase (Fig. 7C). Thus, these complexes are candidates for the activity responsible for alterations in the genomic footprint at the overlapping E2F sites during the cell cycle. However, gel mobility shift experiments do not duplicate the chromatin environment of the endogenous *dhfr* gene and therefore may not accurately reflect changes in E2F binding to the native promoter. The identification of the constituents of complexes A through E and reconstruction of the genomic footprints with purified factors in vitro may clarify the role of these proteins and the temporal sequence of their activities during the cell cycle.

Other protein-DNA interactions at the *dhfr* promoter. The results of genomic footprinting experiments presented here also indicate that certain protein-DNA interactions suggested by in vitro studies to be important for regulating *dhfr* transcription may not be physiologically relevant since they were not detected in CHOC 400 cells at any point in the cell cycle. It is unlikely that discrepancies between in vitro and genomic footprinting analyses are due to amplification of the *dhfr* domain since growth-dependent regulation of the *dhfr* gene was maintained in CHOC 400 cells and complete saturation of Sp1, c-Myc, and other protein binding sites in *dhfr* amplicons was consistently observed. Thus, one benefit of genomic footprinting is discrimination between interactions that occur in cells and those that are detected by DNA binding or transcription assays in vitro. For example, in vitro transcription assays suggest that the first exon of the murine *dhfr* gene contains an enhancer element (22). However, the hamster promoter does not contain this enhancer sequence (59), and no protein binding is evident in CHOC 400 cells within exon 1 at any time in the cell cycle. Similarly, protein-DNA interactions that have been attributed to AP2, AP3, and CTF by in vitro footprinting assays (64) are not detected in CHOC 400 cells. Although methotrexate and other antimetabolites have been reported to stimulate the transcription of *dhfr* (21), the incubation of cells in 200 μg of methotrexate per ml for 24 h had no perceptible effect on the genomic footprint of the major promoter region (data not shown). Finally, besides protein interactions with known promoter elements, the only prominent protein-DNA interaction we observed from the end of exon 1 of the *dhfr* gene to the downstream border of the minor promoter occurred within the first intron of the *rep3* gene. The identity and function of the protein(s) that protects 37 bp of the first *rep3* intron are unknown.

The transcription initiation complex at the minor promoter. In addition to the footprint from the transcription initiation complex at the major *dhfr* promoter, a second large region of protection over the cluster of consensus Sp1 sites and two putative c-Myc binding sites located at positions −480 through −464 in the minor promoter is observed. The features of the genomic footprint of the minor promoter show little variation in the cell cycle. The upstream minor promoter region has little effect on *dhfr* transcription in transient-transfection assays (see the introduction) and most likely functions primarily to regulate the transcription of a class of short *rep3* transcripts that lack the conserved *rep3* exon between the major and minor promoters. It is interesting that the two clusters of Sp1 sites in the major and minor promoter regions are oriented in opposite directions and that each contains an additional transcription factor bound about 20 to 25 bp downstream of the Sp1 cluster. At the major promoter, a protein factor is constitutively bound at the E2F site about 25 bp from Sp1 site 1, whereas at the minor promoter, a protein factor is constitutively bound at c-Myc consensus sequences about 20 bp from Sp1 site 8. Both the c-Myc and E2F sites correspond to transcription start sites, suggesting that the proteins bound at these sites must be involved directly or indirectly in the recruitment of TBP and RNA Pol II to the promoter. Interestingly, E2F-1 has been shown to bind TBP in vitro (31) and c-Myc has been shown to interact directly with general transcription factors (57). In contrast to the E2F sites at the major promoter, however, occupancy of c-Myc site 2 in the minor promoter shows little change in the cell cycle.

The high degree of conservation of the major and minor promoter regions, including the preservation of a *rep3* exon located between the two promoter regions, suggests that coordinate control of *rep3* and *dhfr* gene expression is important. Although *rep3* transcripts increase slightly during the G_1-to-S phase transition (14, 45), the two genes are not controlled in identical fashions. The level of at least one 4.0-kb *rep3* transcript from the major promoter increases threefold after 24 h of serum deprivation, whereas the levels of *dhfr* transcripts decrease during the same time (49). Since *rep3* encodes a homolog of the mismatch DNA repair protein MutS, the intricate organization of the promoter region may be related to different requirements for coordinating *rep3* and *dhfr* transcription during cell proliferation and DNA repair responses.

Nuclease-hypersensitive sites map to protein binding sites. A number of studies have used indirect end labeling and other low-resolution techniques to study the chromatin structure of the *dhfr-rep3* promoter region (3, 49, 52, 61). Two major DNase I-hypersensitive sites in this region are centered at about −55 and −570 (49), which correspond to the locations of the overlapping E2F sites and c-Myc site 2. A minor DNase I-hypersensitive site centered at about −195 corresponds to the upstream edge of the footprint at Sp1 site 4 (49), at which transcription of the 4.0-kb *rep3* transcript from the major promoter begins (45). Thus, the primary transcription initiation sites of both the major and minor promoters are accessible to nuclease in permeabilized cells or chromatin. An additional minor DNase I-hypersensitive site maps to position −415 (49, 61), which coincides with the factor bound to *rep3* intron 1. Although our work does not specifically address the distribution of nucleosomes in the *dhfr* promoter region, others have reported that much of the region is nucleosome free (52, 61). Additional studies have suggested that DNA-binding proteins induce the phasing of nucleosomes in limited portions of this region (61). Under our footprinting conditions, nucleosomes apparently do not interfere with detailed examination of the interactions of protein factors with specific DNA sequences.

In summary, we have used high-resolution genomic footprinting to generate a detailed picture of protein-DNA inter-

actions at two TATA-less promoters during the cell cycle. These studies indicate that multiple species of E2F may control *dhfr* gene transcription, a notion reinforced by examination of E2F DNA binding activity in vitro. We suggest that CHOC 400 cells provide a tractable experimental system for examining the influence of regulatory proteins on protein-DNA interactions and promoter activity at the endogenous *dhfr* promoter within the cell. In particular, this system may provide a useful approach for assessing the sequence of events involving E2F and the retinoblastoma protein family at an endogenous cellular promoter during the cell cycle.

ACKNOWLEDGMENTS

We thank David Pederson and members of the Heintz lab for valuable discussions and comments on the manuscript, Randy Kaufmann for plasmid ΔVa-pMT2, and Gray Crouse for plasmid pGC1587.

J.W. and P.H. were supported by an Environmental Pathology Training grant from the NIEHS. N.H.H. was supported in part by an American Cancer Society Research Faculty Award and the J. Walter Juckett Scholar Award from the Vermont Cancer Center and the Lake Champlain Cancer Research Organization. This work was supported by an NIH grant to N.H.H.

REFERENCES

1. **Araki, E., T. Murakami, T. Shirotani, F. Kanai, Y. Shinohara, F. Shimada, M. Mori, M. Shichiri, and Y. Ebina.** 1991. A cluster of four Sp1 binding sites required for efficient expression of the human insulin gene. J. Biol. Chem. **266:**3944–3948.
2. **Azizkhan, J. C., D. E. Jensen, A. J. Pierce, and M. Wade.** 1993. Transcription from TATA-less promoters: dihydrofolate reductase as a model. Crit. Rev. Eukaryotic Gene Expr. **3:**229–254.
3. **Azizkhan, J. C., J. P. Vaughn, R. J. Christy, and J. L. Hamlin.** 1986. Nucleotide sequence and nuclease hypersensitivity of the Chinese hamster dihydrofolate reductase gene promoter region. Biochemistry **25:**6228–6236.
4. **Bandara, L. R., V. M. Buck, M. Zamanian, L. H. Johnston, and N. B. La Thangue.** 1993. Functional synergy between DP-1 and E2F-1 in the cell cycle-regulating transcription factor DRTF1/E2F. EMBO J. **12:**4317–4324.
5. **Beijersbergen, R. L., R. M. Kerkhoven, L. Zhu, L. Carlee, P. M. Voorhoeve, and R. Bernards.** 1994. E2F-4, a new member of the E2F gene family, has oncogenic activity and associates with p107 in vivo. Genes Dev. **8:**2680–2690.
6. **Blake, M. C., and J. C. Azizkhan.** 1989. Transcription factor E2F is required for efficient expression of the hamster dihydrofolate reductase gene in vitro and in vivo. Mol. Cell. Biol. **9:**4994–5002.
7. **Blake, M. C., R. C. Jambou, A. G. Swick, J. W. Kahn, and J. C. Azizkhan.** 1990. Transcriptional initiation is controlled by upstream GC-box interactions in a TATAA-less promoter. Mol. Cell. Biol. **10:**6632–6641.
8. **Cao, L., B. Faha, M. Dembski, L.-H. Tsai, E. Harlow, and N. Dyson.** 1992. Independent binding of the retinoblastoma protein and p107 to the transcription factor E2F. Nature (London) **355:**176–179.
9. **Chellappan, S. P., S. Hiebert, M. Mudryj, J. M. Horowitz, and J. R. Nevins.** 1991. The E2F transcription factor is a cellular target for the RB protein. Cell **65:**1053–1061.
10. **Chen, J., and D. S. Pederson.** 1993. A distal heat shock element promotes the rapid response to heat shock of the HSP26 gene in the yeast *Saccharomyces cerevisiae*. J. Biol. Chem. **268:**7442–7448.
11. **Chen, X., J. C. Azizkhan, and D. C. Lee.** 1992. The binding of transcription factor Sp1 to multiple sites is required for maximal expression from the rat transforming growth factor alpha promoter. Oncogene **7:**1805–1815.
12. **Ciudad, C. J., A. E. Morris, C. Jeng, and L. A. Chasin.** 1992. Point mutational analysis of the hamster dihydrofolate reductase minimum promoter. J. Biol. Chem. **267:**3650–3656.
13. **Cobrinik, D., P. Whyte, D. S. Peeper, T. Jacks, and R. A. Weinberg.** 1993. Cell cycle-specific association of E2F with the p130 E1A-binding protein. Genes Dev. **7:**2392–2404.
14. **Crouse, G. F., E. J. Leys, R. N. McEwan, E. G. Frayne, and R. E. Kellems.** 1985. Analysis of the mouse *dhfr* promoter region: existence of a divergently transcribed gene. Mol. Cell. Biol. **5:**1847–1858.
15. **DeGregori, J., T. Kowalik, and J. R. Nevins.** 1995. Cellular targets for activation by the E2F1 transcription factor include DNA synthesis- and G_1/S-regulatory genes. Mol. Cell. Biol. **15:**4215–4224.
16. **Devoto, S. H., M. Mudryj, J. Pines, T. Hunter, and J. R. Nevins.** 1992. A cyclin A-protein kinase complex possesses sequence-specific DNA binding activity: p33cdk2 is a component of the E2F-cyclin A complex. Cell **68:**167–176.
17. **Diffley, J. F. X., J. H. Cocker, S. J. Dowell, and A. Rowley.** 1994. Two steps in the assembly of complexes at yeast replication origins in vivo. Cell **78:**303–316.
18. **Dijkwel, P. A., and J. L. Hamlin.** 1992. Initiation of DNA replication in the dihydrofolate reductase locus is confined to the early S period in CHO cells synchronized with the plant amino acid mimosine. Mol. Cell. Biol. **12:**3715–3722.
19. **Dynlacht, B. D., O. Flores, J. A. Lees, and E. Harlow.** 1994. Differential regulation of E2F trans-activation by cyclin/cdk2 complexes. Genes Dev. **8:**1772–1786.
20. **Dyson, N., M. Dembski, A. Fattaey, C. Ngwu, M. Ewen, and K. Helin.** 1993. Analysis of p107-associated proteins: p107 associates with a form of E2F that differs from pRB-associated E2F-1. J. Virol. **67:**7641–7647.
21. **Eastman, H. B., A. G. Swick, M. C. Schmitt, and J. C. Azizkhan.** 1991. Stimulation of dihydrofolate reductase promoter activity by antimetabolic drugs. Proc. Natl. Acad. Sci. USA **88:**8572–8576.
22. **Farnham, P. J., and A. L. Means.** 1990. Sequences downstream of the transcription initiation site modulate the activity of the murine dihydrofolate reductase promoter. Mol. Cell. Biol. **10:**1390–1398.
23. **Farnham, P. J., and R. T. Schimke.** 1985. Transcriptional regulation of mouse dihydrofolate reductase in the cell cycle. Mol. Cell. Biol. **6:**365–371.
24. **Farnham, P. J., and R. T. Schimke.** 1986. Murine dihydrofolate reductase transcripts through the cell cycle. Mol. Cell. Biol. **6:**2392–2401.
25. **Farnham, P. J., and R. T. Schimke.** 1986. In vitro transcription and delimitation of promoter elements of the murine dihydrofolate reductase gene. Mol. Cell. Biol. **6:**2392–2401.
26. **Farnham, P. J., J. E. Slansky, and R. Kollmar.** 1993. The role of E2F in the mammalian cell cycle. Biochim. Biophys. Acta **1155:**125–131.
27. **Ginsberg, D., G. Vairo, T. Chittenden, Z.-X. Xiao, G. Xu, K. L. Wydner, J. A. DeCaprio, J. B. Lawrence, and D. M. Livingston.** 1994. E2F-4, a new member of the E2F transcription factor family, interacts with p107. Genes Dev. **8:**2665–2679.
28. **Girling, R., L. R. Bandara, E. Ormondroyd, E. W.-F. Lam, S. Kotecha, T. Mohun, and N. B. La Thangue.** Molecular characterization of Xenopus laevis DP proteins. Mol. Biol. Cell **5:**1081–1092.
29. **Girling, R., J. F. Partridge, L. R. Bandara, N. Burden, N. F. Totty, J. J. Hsuan, and N. B. La Thangue.** 1993. A new component of the transcription factor DRTF1/E2F. Nature (London) **362:**83–87.
30. **Goldsmith, M. E., and K. H. Cowan.** 1988. Modulation of a human dihydrofolate reductase minigene following release from amino acid deprivation involves both 5′ and 3′ nucleotide sequences. Mol. Pharmacol. **33:**378–383.
31. **Hagemeier, C., A. Cook, and T. Kouzarides.** 1993. The retinoblastoma protein binds E2F residues required for activation in vivo and TBP binding in vitro. Nucleic Acids Res. **21:**4998–5004.
32. **Helin, K., J. A. Lees, M. Vidal, N. Dyson, E. Harlow, and A. Fattaey.** 1992. A cDNA encoding a pRB-binding protein with properties of transcription factor E2F. Cell **70:**337–350.
33. **Helin, K., C. L. Wu, A. R. Fattaey, J. A. Lees, B. D. Dynlacht, C. Ngwu, and E. Harlow.** 1993. Heterodimerization of the transcription factors E2F-1 and DP-1 leads to cooperative trans-activation. Genes Dev. **7:**1850–1861.
34. **Hsiao, K.-M., S. L. McMahon, and P. J. Farnham.** 1994. Multiple DNA elements are required for the growth regulation of the mouse *E2F1* promoter. Genes Dev. **8:**1526–1537.
35. **Huber, H. E., G. Edwards, P. J. Goodhart, D. R. Patrick, P. S. Huang, M. Ivey-Hoyle, S. F. Barnett, A. Oliff, and D. C. Heimbrook.** 1993. Transcription factor E2F binds DNA as a heterodimer. Proc. Natl. Acad. Sci. USA **90:**3525–3529.
36. **Ivey-Hoyle, M., R. Conroy, H. E. Huber, P. J. Goodhart, A. Oliff, and D. C. Heimbrook.** 1993. Cloning and characterization of E2F-2, a novel protein with the biochemical properties of transcription factor E2F. Mol. Cell. Biol. **13:**7802–7812.
37. **Johnson, D. G., K. Ohtani, and J. R. Nevins.** 1994. Autoregulatory control of *E2F1* expression in response to positive and negative regulators of cell cycle progression. Genes Dev. **8:**1514–1525.
38. **Johnson, L. F., C. L. Fuhrman, and L. M. Wiedemann.** 1978. Regulation of dihydrofolate reductase gene expression in mouse fibroblasts during the transition from the resting to growing state. J. Cell. Physiol. **97:**397–406.
39. **Kadonaga, J. T., K. R. Carner, F. R. Masiarz, and R. Tijan.** 1987. Isolation of cDNA encoding transcription factor Sp1 and functional analysis of the DNA binding domain. Cell **51:**1079–1090.
40. **Kaelin, W. G., Jr., W. Krek, W. R. Sellers, J. A. DeCaprio, F. Ajchenbaum, C. S. Fuchs, T. Chittenden, Y. Li, P. J. Farnham, M. A. Blanar, D. M. Livingston, and E. K. Fleming.** 1992. Expression cloning of a cDNA encoding a retinoblastoma-binding protein with E2F-like properties. Cell **70:**351–364.
41. **Krek, W., M. E. Ewen, S. Shirodkar, Z. Arany, W. G. Kaelin, Jr., and D. M. Livingston.** 1994. Negative regulation of the growth-promoting transcription factor E2F-1 by a stably bound cyclin A-dependent protein kinase. Cell **78:**161–172.
42. **La Thangue, N. B.** 1994. DRTF1/E2F: an expanding family of heterodimeric transcription factors implicated in cell-cycle control. Trends Biochem. Sci. **19:**108–114.
43. **Lees, E., B. Faha, V. Dulic, S. I. Reed, and E. Harlow.** 1992. Cyclin E/cdk2 and cyclin A/cdk2 kinases associate with p107 and E2F in a temporally distinct manner. Genes Dev. **6:**1874–1885.

44. **Lees, J. A., M. Saito, M. Vidal, M. Valentine, T. Look, E. Harlow, N. Dyson, and K. Helin.** 1993. The retinoblastoma protein binds to a family of E2F transcription factors. Mol. Cell. Biol. **13:**7813–7825.
45. **Linton, J. P., J.-Y. J. Yen, E. Selby, Z. Chen, J. M. Chinsky, K. Liu, R. E. Kellems, and G. F. Crouse.** 1989. Dual bidirectional promoters at the mouse *dhfr* locus: cloning and characterization of two mRNA classes of the divergently transcribed *Rep-1* gene. Mol. Cell. Biol. **9:**3058–3072.
46. **McGrogan, M., C. C. Simonsen, D. T. Smouse, P. J. Farnham, and R. T. Schimke.** 1985. Heterogeneity at the 5′ termini of mouse dihydrofolate reductase mRNAs. J. Biol. Chem. **260:**2307–2314.
47. **Means, A. L., J. E. Slansky, S. L. McMahon, M. W. Knuth, and P. J. Farnham.** 1992. The HIP1 binding site is required for growth regulation of the dihydrofolate reductase gene promoter. Mol. Cell. Biol. **12:**1054–1063.
48. **Milbrandt, J. D., N. H. Heintz, W. C. White, S. M. Rothman, and J. L. Hamlin.** 1981. Methotrexate-resistant Chinese hamster ovary cells have amplified a 135-kilobase-pair region that includes the gene for dihydrofolate reductase. Proc. Natl. Acad. Sci. USA **78:**6042–6047.
49. **Mitchell, P. J., A. M. Carothers, J. H. Han, J. D. Harding, E. Kas, L. Venolia, and L. A. Chasin.** 1986. Multiple transcription start sites, DNase I-hypersensitive sites, and an opposite-strand exon in the 5′ region of the CHO *dhfr* gene. Mol. Cell. Biol. **6:**425–440.
50. **Mudryj, M., S. H. Devoto, S. W. Hiebert, T. Hunter, J. Pines, and J. R. Nevins.** 1991. Cell cycle regulation of the E2F transcription factor involves an interaction with cyclin A. Cell **65:**1243–1253.
51. **Neuman, E., E. K. Flemington, W. R. Sellers, and W. G. Kaelin, Jr.** 1994. Transcription of the E2F-1 gene is rendered cell cycle dependent by E2F DNA-binding sites within its promoter. Mol Cell. Biol. **14:**6607–6615.
52. **Pemov, A., S. Bavykin, and J. L. Hamlin.** 1995. Proximal and long-range alterations in chromatin structure surrounding the Chinese hamster dihydrofolate reductase promoter. Biochemistry **34:**2381–2392.
53. **Pfeifer, G. P., and A. D. Riggs.** 1991. Chromatin differences between active and inactive X-chromosomes revealed by genomic footprinting of permeabilized cells using DNase I and ligation mediated PCR. Genes Dev. **5:**1102–1113.
54. **Pierce, A. J., R. C. Jambou, D. E. Jensen, and J. C. Azizkhan.** 1992. A conserved DNA structural control element modulates transcription of a mammalian gene. Nucleic Acids Res. **20:**6583–6587.
55. **Potter, M., K. K. Sanford, R. Parshad, R. E. Tarone, F. M. Price, B. Mock, and K. Huppi.** 1988. Genes on chromosomes 1 and 4 in the mouse are associated with repair of radiation-induced chromatin damage. Genomics **2:** 257–262.
56. **Pugh, B. F., and R. Tjian.** 1991. Transcription from a TATA-less promoter requires a multisubunit TFIID complex. Genes Dev. **5:**1935–1945.
57. **Roy, A. L., C. Carruthers, T. Gutjahr, and R. G. Roeder.** 1993. Direct role for Myc in transcription initiation mediated interactions by TFII-I. Nature (London) **365:**359–361.
58. **Santiago, C., M. Collins, and L. F. Johnson.** 1984. In vitro and in vivo analysis of the control of dihydrofolate reductase gene transcription in serum-stimulated mouse fibroblasts. J. Cell. Physiol. **118:**79–86.
59. **Schilling, L. J., and P. J. Farnham.** 1994. Transcriptional regulation of the *dihydrofolate reductase*/rep3 locus. Crit. Rev. Eukaryotic Gene Expr. **4:**19–53.
60. **Schilling, L. J., and P. J. Farnham.** 1989. Identification of a new promoter upstream of the murine dihydrofolate reductase gene. Mol. Cell. Biol. **9:** 4568–4570.
61. **Shimada, T., K. Inokuchi, and A. W. Nienhuis.** 1986. Chromatin structure of the human dihydrofolate reductase gene promoter. J. Biol. Chem. **261:** 1445–1452.
62. **Shull, S., N. H. Heintz, M. Perisamy, M. Manohar, Y. M. W. Janssen, J. P. Marsh, and B. T. Mossman.** 1991. Differential regulation of antioxidant enzymes in response to oxidants. J. Biol. Chem. **266:**24398–24403.
63. **Slansky, J. E., Y. Li, W. G. Kaelin, and P. J. Farnham.** 1993. A protein synthesis-dependent increase in E2F1 mRNA correlates with growth regulation of the dihydrofolate reductase promoter. Mol. Cell. Biol. **13:**1610–1618.
64. **Smith, M. L., P. J. Mitchell, and G. F. Crouse.** 1990. Analysis of the mouse *Dhfr*/*Rep-3* major promoter region by using linker-scanning and internal deletion mutations and DNase I footprinting. Mol. Cell. Biol. **10:**6003–6012.
65. **Stubblefield, E., and R. Klevecz.** 1965. Synchronization of Chinese hamster cells by reversal of colcemid inhibition. Exp. Cell Res. **40:**660–664.
66. **Swick, A. G., M. C. Blake, J. W. Kahn, and J. C. Azizkhan.** 1989. Functional analysis of GC element binding and transcription in the hamster dihydrofolate reductase gene promoter. Nucleic Acids Res. **17:**9291–9303.
67. **Wade, M., M. C. Blake, R. C. Jambous, K. Helin, E. Harlow, and J. C. Azizkhan.** 1995. An inverted repeat motif stabilizes binding of E2F and enhances transcription of the dihydrofolate reductase gene. J. Biol. Chem. **270:**9783–9791.
68. **Weintraub, S. J., K. N. B. Chow, R. X. Luo, S. H. Zhang, S. He, and D. C. Dean.** 1995. Mechanism of active transcriptional repression by the retinoblastoma protein. Nature (London) **375:**812–815.
68a. **Wells, J., and N. H. Heintz.** Unpublished data.
68b. **Wells, J., J. Magae, S. Illenye, and N. H. Heintz.** Unpublished data.
69. **Wiley, S. R., R. J. Kraus, and J. E. Mertz.** 1992. Functional binding of the "TATA" box binding component of transcription factor TFIID to the −30 region of TATA-less promoters. Proc. Natl. Acad. Sci. USA **89:**5814–5818.
70. **Wu, C.-L., L. R. Zukerberg, C. Ngwu, E. Harlow, and J. A. Lees.** 1995. In vivo association of E2F and DP family proteins. Mol. Cell. Biol. **15:**2536–2546.
71. **Zawel, L., and D. Reinberg.** 1993. Initiation of transcription by RNA polymerase II: a multistep process. Prog. Nucleic Acid Res. Mol. Biol. **44:**67–108.
72. **Zhu, L., L. Zhu, E. Xie, and L.-S. Chang.** 1995. Differential roles of two tandem E2F sites in repression of the human p107 promoter by retinoblastoma and p107 proteins. Mol. Cell. Biol. **15:**3552–3562.